Desalination and Water Treatment
www.deswater.com
15 (2010) 92–107
March
1944-3994 / 1944-3986 © 2010 Desalination Publications. All rights reserved.
doi: 10.5004/dwt.2010.1672

Review of seawater natural organic matter fouling and reverse osmosis transport modeling for seawater reverse osmosis desalination

Monruedee Moonkhum[a], Young Geun Lee[a], Yun Seok Lee[a], Joon Ha Kim[a,b,c]*

[a]*Department of Environmental Science and Engineering,* [b]*Center for Seawater Desalination Plant,*
[c]*Sustainable Water Resource Technology Center, Gwangju Institute of Science and Technology, Gwangju, 500-712, Korea*
Tel. +82 (62) 970-3277; Fax +82 (62) 970-2434; email: joonkim@gist.ac.kr

Received 12 November 2009; Accepted in revised form 24 December 2009

ABSTRACT

To date, over 80 papers on transport modeling and natural organic matter (NOM) relating to seawater reverse osmosis (SWRO), have been reviewed. As a result of such focus, NOM, one of the main foulants related to reverse osmosis (RO) membranes, has been shown to possess intrinsic chemical complexities and ambiguities, necessitating further investigation. Consequently, since such NOM fouling and transport mechanisms associated with SWRO are not fully understood, a summation of previous studies has been included in the paper in question to systematize information, not only as to RO membrane transport modeling, but NOM fouling characteristics, as well. Accordingly, RO transport models in the review are classified into three categories: diffusion-based, pore, and irreversible thermodynamic models. In addition, specific features, unique assumptions, and applications for each model are examined. The paper consists of the following components towards meaningful understanding of NOM fouling model development during SWRO: 1) SWRO fundamentals as to membranes, 2) NOM fundamentals as to seawater, 3) RO transport modeling theories, 4) conclusion, and 5) future directions of NOM fouling model development.

Keywords: Natural organic matter (NOM); Seawater reverse osmosis (SWRO); Membrane transport models; Fouling mechanism

1. Introduction

Desalination processes have emerged as an effective solution for solving potable water shortages, quickly emerging as a major global problem [1,2]. Especially, seawater reverse osmosis (SWRO) membrane desalination, in relation to thermal desalination, e.g., multistage flash desalination (MSF) and multi-effect distillation (MED), is more technologically feasible in reducing energy consumption during fresh water conversion [3]. Apart from such merits, membrane fouling during SWRO application persists as a major impediment, reducing operation efficiency during filtration process.

Reverse osmosis (RO) membrane fouling is classified according to the following foulant types: particle/colloidal, biological, inorganic (scaling), and organic fouling [4]. Particularly, natural organic matter (NOM) fouling has emerged as a focal point in research and application, playing a key role in irreversible fouling generation during SWRO desalination. Contrary to reversible fouling, easily cleaned by back washing, irreversible fouling requires chemical cleaning due to permanent bonding of organic matter and other foulants (e.g., inorganic matter and colloids) [4,5]. However, fundamental NOM fouling mecha-

* Corresponding author.

Presented at SeaHERO Academic Workshop on Development and Optimization of SWRO Desalination Systems
Korea University, Seoul, Korea, November 13–14, 2009

nisms have not been fully understood due to possessing a complex mix of particulate and soluble components, both inorganic and organic matters, distinguishing such mechanisms from a variety of other sources [6].

Most previous studies dealing with SWRO desalination models have avoided focusing on NOM fouling, rather centering on general mass transport modeling. Moreover, a variety of theoretical RO transport models have tended to be directed towards underlying membrane separation mechanisms as well as membrane property influences, combined with operational effects relating to salt rejection [7–9]. Generally, such models were developed under general aspect; however, the inclusion of specific RO transport models dealing with NOM fouling was overlooked, failing to prevent and reduce serious fouling during SWRO application. Conversely, the paper in question is focused not only on fundamental aspects of RO application and NOM via corresponding fouling mechanisms, but on RO transport model theories, as well. Furthermore, future directions and approaches in developing reasonable NOM fouling and SWRO models are addressed in the final section.

2. Fundamentals of seawater reverse osmosis desalination

2.1. Seawater

Common seawater consists of 96% water, the remaining 4% of the total dissolved solids (TDS). Seawater TDS mainly consist of inorganic ion compositions, approximately 0.002–0.004% of TDS representing organic matter [10,11]. In general, average seawater salinity represents about 35% of the total weight [12] ranging from 32 to 40% of total weight in the open sea [13]. Ocean salinity varies according to freshwater input (e.g., precipitation and river/groundwater runoff), seawater evaporation rate, and seawater temperature [13]. Table 1 demonstrates the effects of temperature on salinity, revealing higher TDS during exposure to higher temperatures due to increased seawater constituent solubility [12].

Chloride and sodium ions are considered major seawater components, overall seawater composition being demonstrated in Fig. 1 [12]. Accordingly, widespread problems during SWRO application result in high energy input and the necessity of clean-up application. Specifically, scaling from inorganic materials and complex fouling from organic matters mixes with microorganisms. Such difficulties have profound effects during reverse osmosis application, i.e., decreased performance and productivity, as well as increased production costs [14,15].

Table 1
Salinity and temperature of various seawater sources [12]

Seawater source	TDS (mg/L)	Avg. temperature (°C)
Pacific/Atlantic Ocean	33,500	18
Caribbean	36,000	26
Mediterranean	38,000	26
Gulf of Oman, Indian Ocean	40,000	30
Red Sea	41,000	28
Arabian Gulf	45,000	26

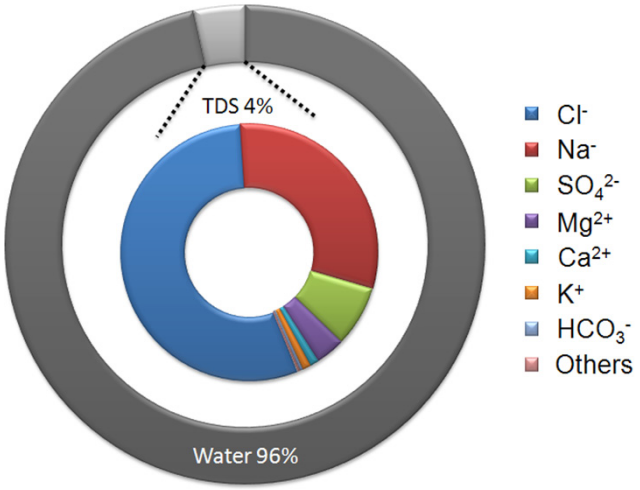

Fig. 1. Concentration of major seawater ions (ppt by weight), adapted from [9].

2.2. Seawater reverse osmosis process

Desalination is a purification process, converting common seawater into pure potable water. Generally, three groups of desalination technology exists: MSF, electrodialysis, and RO process. Among such technologies, RO process represents the most popular and widely used technique due to lower energy consumption [10]. Further, the RO process offers promising treatment for seawater desalination, including high water pressure application across membranes, as well as forced feeding through opposite membrane sites [10]. Since such membranes possess a unique property, i.e. semi-permeability [10], which possible permeates for water not sea salts [16]. Standard pressure during seawater desalination commonly requires a high range of 55–68 bar [17]. Factors affecting process performance, such as feed water composition and membrane properties, are usually selected as parameters towards maximizing process effectiveness. However, membrane surface properties have represented the primary focus in previous studies due to ease of control [18]. Initially, membrane material development commenced with the use of ceramic membranes discovered by Pfeffer and colleagues in the 1850s [16]. Afterwards, Reid and Breton developed the use of cellulose acetate films in 1959 [19]. Such films measured 5–20 μm in thickness, resulting in very low permeate fluxes. However, by

applying high pressure on the feed solution, up to 69 bar, the membranes were capable of eliminating over 98% of existing salt. Recently, cellulose acetate membranes, developed by Loeb–Sourirajan, have been able to operate 10 times faster than Reid and Breton's membrane, while maintaining the same rejection rate performance. Such innovation hastens effective development of RO technology [16].

SWRO application includes the following processes: seawater intake, pre-treatment, RO membrane, and post-treatment [4,20]. SWRO application commences during feed water containment from the sea via coast and beach wells, or open seawater intake systems [21]. Subsequently, intake water condition is further adjusted as to pH value, afterward being exposed to pre-treatment in order to separate particulate matter. At the end of the pre-treatment process, antifoulants are added to prevent fouling. Afterwards, treated water is pumped to RO membranes by means of high water pressure. Finally, pure water is re-mineralized, re-hardened, disinfected by chlorination, finally meeting drinking water standards [10]. Fig. 2 demonstrates the schematics of general SWRO application.

2.3. RO membrane performance determination

SWRO performance is influenced by the correlation of several factors including feed water quality, operating conditions, membrane characteristics, concentration polarization, as well as foulant characteristics and fouling mechanisms [22,23]. The major governing factors determining RO performance include membrane properties (i.e. membrane material chemistry and physical structure) and fouling development. Membrane surface properties are directly affected filtration efficiency. However, supplementary parameters, including membrane pore dimension, barrier layer thickness, and elemental composition, are ideally considered in order to provide accurate, precise, and effective evaluation [24,25]. Additionally, permeate flux and solute rejection rates, due to simplicity and speed of onsite measurement, are key factors in determining efficacy. In order to maximize efficiency, developing membranes with specific goals of high foulant resistance, high performance, as well as longevity are vital [23]. Furthermore, a clear understanding of fouling mechanisms, in unison with effective fouling protection or reduction options, ideally advances application.

2.4. Seawater RO fouling

Scaling and fouling are often singled out as phenomena inflicting potentially serious harm during SWRO application. The potential of such harm as to RO membrane fouling is largely dependent upon feed water composition, associated with the accumulation of rejected salts on membrane surface during filtration [10]. Seawater foulants are classified into four categories: inorganic, colloidal, biological, and organic foulants [4]; cause–effects of seawater foulants shown in Table 2. Among all foulants, NOM is capable of generating significant fouling. Since NOM represents a complex mixture of inorganic and organic origins, changing according to environmental conditions (e.g., pH), precise operative mechanisms are largely undiscovered and poorly understood [26].

2.5. RO fouling mechanisms

Generally, RO membranes are assumed to represent non-porous membranes; therefore, adhesion among foulant molecules, as well as between foulants and membrane surfaces, account for dominant fouling mechanisms [28,29]. The sequence of RO membrane fouling initially includes foulant deposition on membrane surfaces due to adhesion forces between foulants and membrane surfaces. Afterwards, critical fouling layers are developed. Subsequently, intermolecular adhesion among bulk and

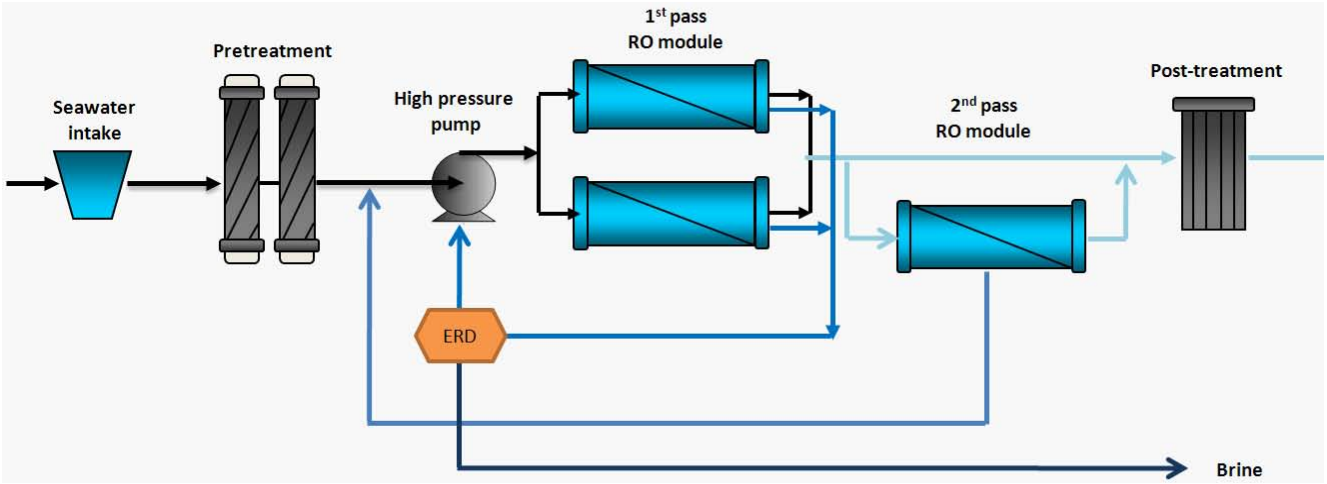

Fig. 2. Schematics of general SWRO processes.

Table 2
Cause–effects of seawater foulants [27]

Foulant	Mechanism	Cause	Effect
Colloidal	Deposition	Accumulation of particles and macromolecules on, in, and near membranes	Creation of additional resistance layers as to permeation
Organic matter (e.g., polyphenolic compounds, proteins, and polysaccharides)	Adsorption	Permeate resistant layer formation via negatively charged functional groups on organic foulants with charged membrane surface affinity	Increased cohesion as to membrane surfaces
		Interaction between organics and microorganisms	Biofilm formation promotion
Inorganic (e.g., iron, silica, aluminum, calcium, phosphorus, and sulfate)	Deposition	Promotion of inorganic matter deposition as to concentration polarization	Salt precipitation and suspension on membrane surfaces, leading to scaling and fouling
Biofouling (e.g., bacteria, algae, and fungi)	Adhesion	Microorganism adhesion and biofilm growth on membrane surfaces	Bacteria enzymatic biodegradation of membrane material reducing membrane longevity

membrane surface-deposited foulants is established on governing mechanisms [28]; in this case, diffusion which represents apparent foulant transport. Conversely, in regards to the molecular facet, RO membrane is assumed as being microporous as well. In such cases, foulant transport not only takes place by means of membrane surface diffusion, but also by convection transport through microporous [27]. For organic fouling, the interaction between foulant-membrane as well as foulant-foulant surfaces is promoted by hydrogen bonding [30]. Additionally, other studies have demonstrated that various organic solutes interact with RO membranes by means of absorption mechanisms [31–33].

3. Fundamentals of NOM in seawater

3.1. Seawater natural organic matter

Although organic matter concentration within seawater is insignificant compared to inorganic constituents, such substances are more acutely problematic during reverse osmosis desalination [10]. Organic matter, by merging with inorganic particles as well as microorganisms, advances the occurrence of irreversible fouling. Consequently, application of higher water pressure as to normal operation, is required to maintain the same rate of permeate flux, necessitating chemical cleaning as well.

Over 60–80% of organic matter dissolved from saltwater is represented by humic substances [26,34]. Humic substances comprise a general class of ubiquitous material found within terrestrial and aquatic environments, further affecting the aesthetic quality of water by imparting a general brown hue [10]. Humic acids are generally thought to substantially harm RO application due to recurrent gel formation, akin to fouling layering, by means of organic compound and multivalent ion integration [10]. The adsorption of such complex organic matters on membrane surfaces results in rapid permeability decline. Moreover, NOM is possibly broken down into smaller fragments during feed water chlorination, thereby loosing inherent inert properties and becoming primary nutrient sources for bacteria. Accordingly, interaction between fragmented organic matter and microorganisms gives rise to critical biofouling. Additionally, such minute NOM particles are transformed into carcinogenic organic compounds being toxic to humans. As a result of such by-products, RO plant operators are obliged to increase operation cost during post-treatment before water is finally distributed [10].

3.2. Chemistry of NOM

NOM chemistry within seawater demonstrates a wide range of molecular weights and functional groups. Such substances are formed by combination of allochthonous as well as autochthonous input. In general, humic substances are differentiated as to hydrophobic and hydrophilic fractions. Hydrophobic NOM fractions, vis-a-vis hydrophilic fractions, are more likely to be absorbed on membrane surfaces. In addition, previous studies have demonstrated that NOM adsorption mechanisms on membrane surfaces increase proportionally as to molecular weight [35,36]. Moreover, divalent ions with high molecular weight NOM, compared to low molecular weight, have been promoted as being more effective in regards to fouling [37].

3.3. Factors affecting NOM fouling

NOM fouling is likely affected by several factors including NOM characteristics (e.g., hydrophobic or hydrophilic), solution chemistry (e.g., pH, temperature and ionic strength), membrane characteristics (e.g., surface charge and morphology) and operating conditions (e.g., permeate flux and velocity) [35]. A diagram of the factors affecting NOM fouling is demonstrated in Fig. 3. Moreover, previous studies have revealed the effects of fouling factors as to seawater NOM fouling, as shown in Table 3.

3.3.1. Physical operating conditions

Operating conditions include permeate flux [4,46–48], pressure [49], and mass transfer properties of fluid boundary layers are considered as factors affecting NOM transport on membrane surface. Further, such operating conditions affect not only fouling efficacy, but characteristics, as well. Accordingly, NOM fouling is controlled by the optimization of such operating conditions.

3.3.2. Solution chemistry

Factors involved in feed solution chemistry, such as ionic strength [47], pH [46,49–52], as well as monovalent and divalent ion concentration [46,50,51,53] represent major factors in NOM absorption acceleration on membrane surfaces. Furthermore, such factors help to introduce electrostatic interaction not only among solutes and membrane surfaces, but exclusively among solutes, as well. In brief, various fouling characteristics are generated by means of solution chemistry diversity.

3.3.3. Membrane properties

Membrane properties also influence fouling potential. Properties such as surface characteristics (e.g., surface roughness, charge, and hydrophobicity) [18], surface structures and surface chemical properties [38,45–47,49,50,] are representative. Accordingly, beneficial characteristics during membrane producing are the following: increased smoothness, increased negative charge, and hydrophobic membrane reduction [18].

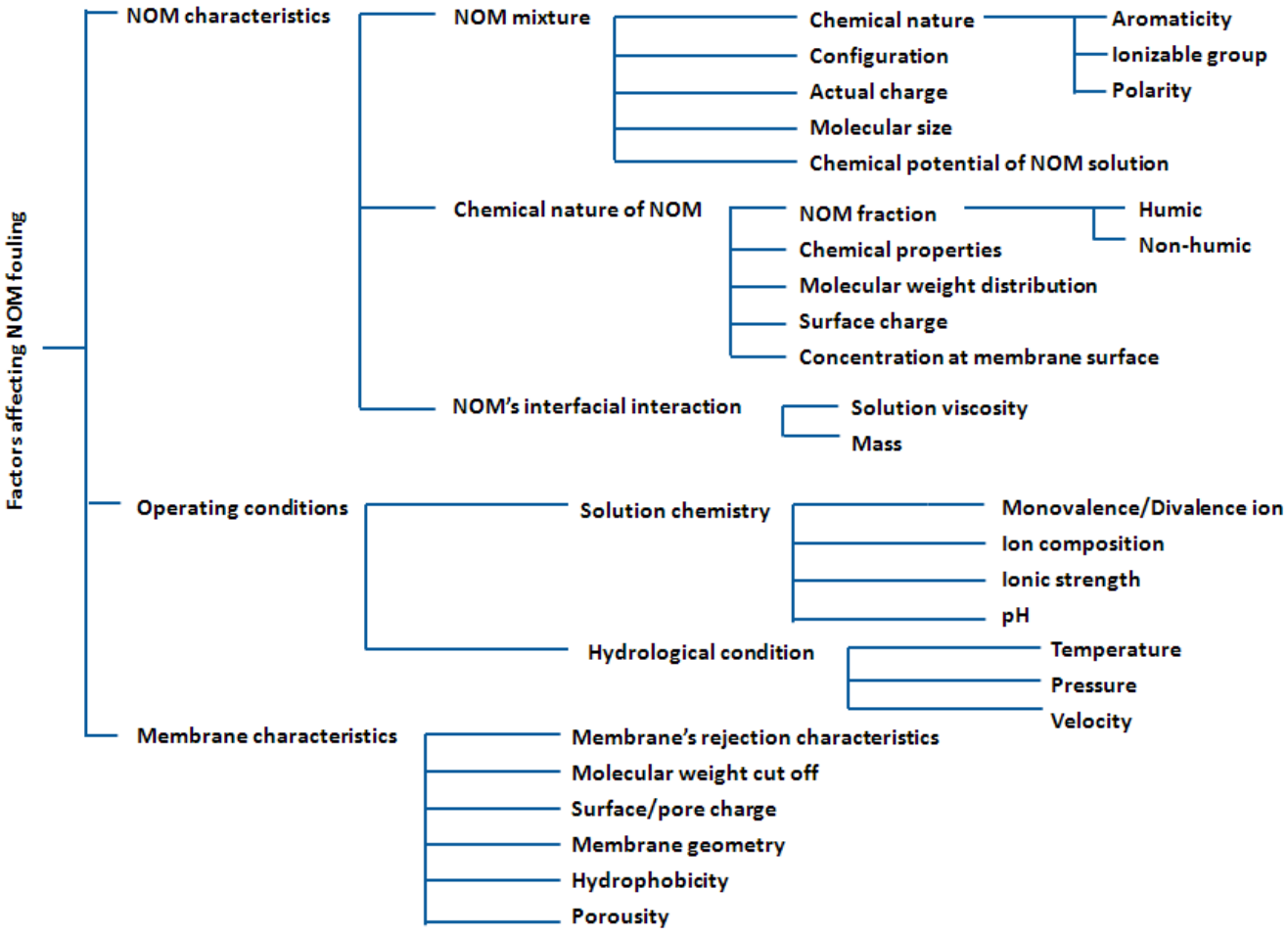

Fig. 3. Diagram of factors affecting NOM fouling.

Table 3
Effects of fouling factors as to seawater NOM fouling

Factor	Parameter	Cause-effect	References
Feed chemistry	Ionic strength	The effects of electrostatic and hydrophobic forces as to fouling shape and characteristics (e.g., dense thick or loose sparse thin fouling layers) impacting permeate production	[38]
	pH	The effects of electrostatic forces on fouling shape and characteristics (e.g., dense thick or loose sparse thin fouling layers) impacting permeate production	[38]
	Pressure	The effects of pressure strength as to fouling layer compaction	[38]
Membrane properties	Roughness	The production of low interaction energy wells due to rougher surfaces resulting in preferential colloidal particle deposits	[39–41]
	Charge	Electrostatic repulsion between evenly charged foulants and membrane surfaces allowing foulant adhesion	[42–44]
	Hydrophobic	More severe impairment of hydrophobic membranes due to membrane fouling as to hydrophilic membrane impairment due to strong hydrophobic interaction, possibly allowing multi-fouling layering on membrane surfaces	[42,50]

4. Theoretical RO membrane transport models

According to existing models, RO transport models are classified into 3 categories based on membrane surface structures (i.e., non-porous, porous, and irreversible thermodynamic-based models) [7]. Since transport mechanisms within membranes are governed by both solvent and solute transports (e.g., diffusion and convection) [54,55] such mechanisms, as well as membrane characteristics and structures, represent vital factors in developing and applying NOM fouling models. For clarification, Fig. 4 demonstrates existing RO transport models. In lieu of ambiguous NOM fouling mechanisms employed during SWRO, e.g., being less developed and effectual than other foulants, further study is required. Likewise, complex and vague NOM properties, as well as minimal concentration within seawater, represent additional sources of concern. Moreover, several unknown fractions and functional groups need to be characterized and identified in order to insure future progress. There-

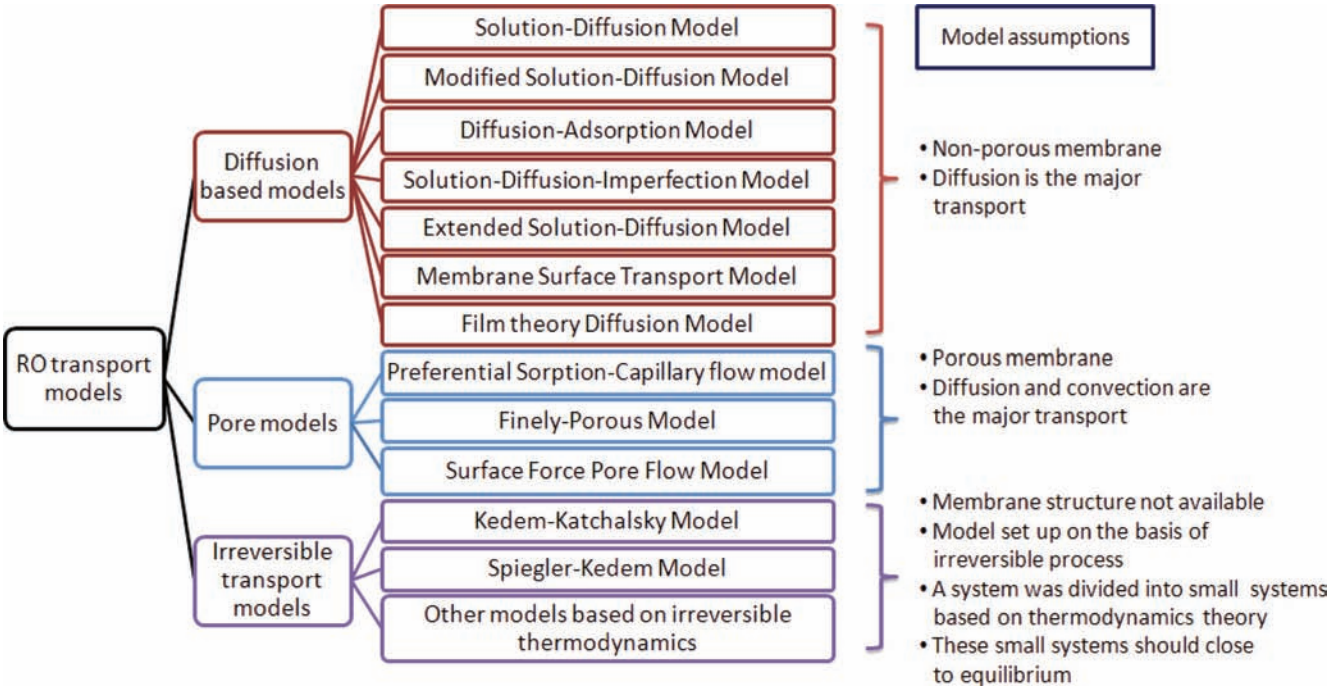

Fig. 4. Diagram of existing RO transport models.

fore, specific models for NOM fouling during SWRO have not been completely developed yet. A number of earlier studies are directed at attempting to modify and apply such models towards NOM fouling prediction, however the majority of the studies reveal that such models fail to predict effectively due to diluted NOM concentration.

4.1. Non-porous models (diffusion-based models)

Diffusion-based models operate under the assumption that RO membranes are non-porous, thus NOM transports, as well as other particles, subsist among interstitial spaces of polymer chains or nodules. Hence, the incidence of diffusion represents evidence of transport, consequently supporting such an assumption. Accordingly, solute flux depends on transmembrane pressure and respective concentration variation across membranes, also known as the molecular chemical potential gradient [29].

4.1.1. Solution–diffusion model

The following simple and popular model is typically applied in order to predict solvent and solute transport during RO when membrane surfaces are assumed to be completely non-porous [27]. Thus, in such a case, only diffusion accounts for transport. As to application, previous studies have applied models in accordance with concentration polarization theory, simulation results revealing robust agreement with experimental results over a range of operating conditions [56]. The governing equations contain the following two crucial coefficients: solvent permeability and solute permeability coefficients [57–58].

The diffusion of water flux during filtration is characterized by:

$$J_w = -D_w \frac{dc_w}{dx} \tag{1}$$

where J_w represents solvent flux due to the chemical potential gradient with respect to membrane, D_w represents the diffusion coefficient of the membrane solvent, and c_w solvent concentration.

However, water flux is also characterized in Eq. (2), during systematic impact due to Henry's Law, the subsequent Eq. (1) becoming:

$$J_w = \frac{D_w c_w}{R_{\text{gas}} T} \frac{d\mu_w}{dx} \simeq \frac{D_w c_w}{R_{\text{gas}} T} \frac{\Delta\mu_w}{\Delta x} \tag{2}$$

where μ_w represents chemical potential of water, R_{gas} gas constant, and T temperature.

Chemical potential represented in Eq. (2) is an immeasurable parameter, being converted to a measureable quantity as to expression Eq. (3).

$$\mu_i(T,P) = \mu_i^0(T,P^0) + R_{\text{gas}} T \ln a_i + \bar{V}_i(P - P^0) \tag{3}$$

where μ_i represents the chemical potential component i, P transmembrane pressure, P_s solute permeability, and $\bar{V}_i$ partial molar volume of component i.

Subsequently, the converted equation [Eq. (3)] is substituted for Eq. (2) to obtain Eq. (4). Such a newly developed equation is practical, since D_w, c_w, and $\bar{V}_w$ are pressure independent.

$$J_w = \frac{D_w c_w \bar{V}_w}{R_{\text{gas}} T \Delta x} (\Delta p - \Delta\pi) \equiv A(\Delta p - \Delta\pi) \tag{4}$$

where $\bar{V}_w$ represents partial molar water volume. The solute flux is expressed according to the concentration gradient, relying on Fick's law as expressed in Eq. (5). In such a case, the solute diffusion coefficient is assumed to be independent from salt membrane concentration (C_s). Although the value for C_s is impossible to gauge, such a value is related to external solution concentration during linkage with distribution coefficient, k_s.

$$J_s = -D_s \frac{dc_s}{dx} \simeq +D_s \frac{\Delta c_s}{\Delta x} \tag{5}$$

$$k_s = \frac{\text{grams solute/cc. membrane}}{\text{grams solute/cc. solution}} \tag{6}$$

where c_s represents local solute concentration per unit membrane volume, and D_s the diffusion coefficient of the membrane solute. As to Eq. (5), at high concentration ($-dc_s/dx$) may not equal ($+\Delta c_s/\Delta x$) due to the concentration profile in membranes not always being linear. Thus, by merging Eq. (5) and Eq. (6), solute flux equation becomes:

$$J_s = -D_s k_s \frac{C_p - C_R}{\Delta x} = K_2(C_R - C_p) \tag{7}$$

where C_p represents permeate concentration, C_R rejection concentration, and K_2 the coupling coefficient with pore flow description. An additional equation also related to particle transport is salt rejection, expressed as:

$$R = 1 - \frac{C_p}{C_R} = 1 - \frac{D_s k_s R_{\text{gas}} T}{D_w c_w \bar{V}_w} \cdot \frac{C_p - C_R}{C_R} \cdot \frac{1}{(\Delta P - \Delta\pi)} \tag{8}$$

Such a limitation renders the model unsuitable for real membrane application due to the microporous structures of surface layers. As mentioned previously, such a model illuminates both solute and solvent transport, relating exclusively to diffusion. Nevertheless, pore flow is significantly impacted by salt transport, as well. Further, the model inadequately portrays water or solute flux as to low water content membranes, especially for various RO membranes and organic matter [7].

4.1.2. Modified solution–diffusion model (steady-state model)

A more reasonable assumption was added to the solution-diffusion model which represents steady-state

fluxes across the membrane. For organics, the total (solute and water) concentration in the membrane should be identified [59]. This implies that both the water and the solute possible to occupy within the membrane. Then water and solute fluxes written as:

$$J_w = \left(\frac{C_{tm} - C_{ms}}{C_{tm}}\right)\frac{C_{tm} D_{wn} \overline{V}_w}{R_g T \delta}(\Delta P - \Delta\pi) = \left(1 - \frac{C_{ms}}{C_{tm}}\right) A^* (\Delta P - \Delta\pi) \quad (9)$$

$$J_s = \frac{D_{sm}}{\delta}(C_{smf} - C_{smp}) \quad (10)$$

where C_{tm} represents the total concentration in the membrane, C_{ms} the membrane solute concentration, D_{wm} the water diffusivity in membrane, $\overline{V}_m$ the partial molar volume of water, R_{gas} the ideal gas constant, and A^* the new permeability constant.

4.1.3. Diffusion–adsorption model (unsteady-state model)

Another modified solution-diffusion model for solutes that are able to adsorb in the membrane pores, the transport behavior can be described by a diffusion-adsorption model. This model assumed that water and solute transport occurs by uncoupled diffusion across the membrane. Solute flux can be described by Fick's law and also the concentration of solute in the membrane can be expressed by adsorption rate [59]. The water and solute fluxes are expressed:

$$\frac{dC_c}{dt} = \frac{A_m J_w C_c - A_m J_w C_P - \frac{dQ_{tm}}{dt}}{V_F(1-r)} \quad (11)$$

$$C_P = \frac{J_s}{J_w} \quad (12)$$

where C_c represents concentrate solute concentration, A_m the membrane surface area, C_P the permeate solute concentration, Q_{tm} the total solute adsorption in membrane, V_F the feed volume, and r the permeate water recovery.

4.1.4. Solution–diffusion–imperfection model

Based on solution diffusion model limitations, the solution diffusion imperfection model was developed to augment such restrictions. Additionally, such a model is applicable for organic solutes by means of a pressure-dependent term [60]. For practical application, the pore flow term is included in the solution diffusion model. Thus, the model is effective during filtration of both surface and porous transport [7,27,61]. Total water and solute flux are represented in Eq. (13) and (14), respectively.

$$N_w = J_w + K_3 \Delta P c_w = A(\Delta P - \Delta\pi) + K_3 \Delta P c_w \quad (13)$$

$$N_s = J_s + K_3 \Delta P C_R = K_2(C_R - C_P) + K_3 \Delta P C_R \quad (14)$$

where N_w represents water flux according to preferential sorption-capillary flow model, K_3 the solute permeability coefficient, A the solvent permeability coefficient in the solution-diffusion model, and N_s total solute flux.

Referring to Eqs. (13) and (14), the permeate velocity is derived accordingly:

$$V_w = K_1(\Delta P - \Delta\pi) + K_3 \Delta P \quad (15)$$

$$V_w C_P = K_2(C_R - C_P) + K_3 \Delta P C_R \quad (16)$$

where V_w represents local water permeation velocity through the membrane, and K_1 the water permeability coefficient. As Eqs. (15) and (16) contain the pressure drop term, useful for rejection computation, the rejection is thus calculated accordingly:

$$R = \{C_R \Delta P(1 + K_3/K_1) + \pi_0(C_R + K_2/K_1) - [C_R^2 \Delta P^2 (1 + K_3/K_1) + 2C_R \Delta P \pi_0 (1 + K_3/K_1) \cdot (C_R + K_2/K_1) \pi_0^2 (C_R + K_2/K_1)^2 - 4\pi_0 \Delta P C_R^2]^{1/2}\} / 2\pi_0 C_R \quad (17)$$

where R represents rejection, and π_0 feed osmotic pressure. However, the model contains two key disadvantages: First, the model relies on parameters that are obtained exclusively by nonlinear regression, used for membrane system characterization. Second, parameters describing such systems usually characterize feed concentration and pressure functions [7]. Furthermore, the application has been shown to dilute particular organic systems ($\Delta\pi = 0$), resulting in substantially lower water fluxes than predicted results [62].

4.1.5. Extended solution–diffusion model

Since the solution diffusion model is divested of possible pressure dependence as to solute chemical potential, the model is also significant for organic solutes. Thus, such a model is enriched by adding the negative solute rejection term [24,60]. Based on the modification, the solute flux is written accordingly:

$$J_s = \frac{D_{sm} K_{sm}}{\delta}(C_F - C_P) + L_{sp} \Delta P \quad (18)$$

The rejection is represented by

$$\frac{1}{R}\left[1 - \frac{L_{sp}}{A C_F}\left(1 - \frac{\Delta\pi}{\Delta P}\right)\right] = 1 + \left[\frac{B}{A(\Delta P - \Delta\pi)}\right] \quad (19)$$

where D_{sm} represents the solute diffusion coefficient in the membrane, K_{sm} the partition coefficient, C_F feed concentration, L_{sp} the phenomenological coefficient, and B the solute permeability coefficient. However, the model has not been widely applied in RO membrane models. Nevertheless, such a model fails to address substantial decreases in water flux for some dilute organic systems [62].

4.1.6. Membrane surface transport model

In the model in question, solute mass transfer between membrane surfaces and cell walls are exclusively taken into account [63]. Subsequently, membranes permeate flux is clarified according to the following relation:

$$J_w = \frac{\Delta P - \Delta\pi}{\mu\left(R_m + R_g + R_{cp}\right)} \tag{20}$$

where μ represents viscosity of solution, R_m membrane resistance, R_{cp} concentration polarization resistance, and finally R_g gel layer resistance.

4.1.7. Film theory diffusion model

Concentration polarization is defined as built-up intensity at membrane-liquid interfaces during filtration. Consequently, such a process, via inclusion of concentration polarization, is very crucial during transport mechanism identification. Characterized by steadiness, solute flux remains constant through films, equaling solute flux through membranes [63].

$$C_P = -D\frac{dC}{dx} + C_i F_w \tag{21}$$

where C_i represents concentration of component *i*.

4.2. Porous models

Apart from the general assumption that RO membranes are non-porous, diffusion, nevertheless, plays an important role during solvent and solute transport. However, real membranes are considered as possessing microporous surfaces. Hence, transport mechanisms not only transpire through dense layers via diffusion, but also include convection as to pores. A variety of transport models have been developed under such assumptions, demonstrated one-by-one accordingly [62].

4.2.1. Preferential sorption–capillary flow model

When membrane surfaces are assumed as microporous and homogenous, membrane surface properties, dimension, and membrane pore quantity combine to play an important role during transport. Subsequently, both preferential sorption and repulsion occurred during membrane interface and solution contact. According to the model in question, coupling of surface phenomena and fluid transport via capillary pores are explained by water transport through viscous flow, solute transport via pore diffusion, and boundary layer development by means of film theories [27,62,64].

During filtration under high water pressure, water tends to be adsorbed onto pore walls, solutes being rejected and fixed on membrane surfaces. Water and salt flux are demonstrated by Eqs. (22) and (23), respectively.

$$N_w = A\left[\Delta P - \left(\pi(X_{s2}) - \pi(X_{s3})\right)\right] \tag{22}$$

$$N_s = \frac{Ck_s D_{sm}}{\delta}(X_{s2}) - (X_{s3}) \tag{23}$$

where N_w represents water flux according to the preferential sorption–capillary flow model, N_s total solute flux, X_{s2} and X_{s2} mole fractions of the solute on high and low pressure membrane sides, respectively, and δ fouling layer thickness. The derivation of such equations is based on the solution diffusion model, in unison with the film theory, related to membrane surface and bulk solution concentrations. Furthermore, both water and solute permeability coefficients are precisely expressed in terms of operating conditions. Solute rejection is represented accordingly:

$$\frac{1}{R} = 1 + \frac{D_{sp}K_D C_T}{\delta}\frac{1}{A\left\{\Delta P - \left[\pi(X_F) - \pi(X_P)\right]\right\}} \tag{24}$$

where D_{sp} represents solute diffusivity in membrane pores, X_F the solute mole fraction in feed water, and X_p the solute mole fraction in permeate. The model has been applied during transport analysis for numerous solutes and membranes, demonstrating that water flux drop caused by various dilute organic particles and solute rejection is not accounted for by such equations [62].

4.2.2. Finely-porous model

Solute and solvent transport is directly affected by membrane surface properties. Most RO membranes consist of asymmetric structures, characterized by imperfect surface layers, such transport mechanisms representing not only diffusion but viscous flow via microporous membranes, as well [29]. Hence, the extended diffusion solution model, by the inclusion of viscous flow, represents a valuable and more accurate application for highly-porous membranes [7.27]. The total volume flux is expressed according to Poiseulle's law:

$$\in u = -\frac{\in r_p^2}{8\mu}\frac{dP}{dx} = + - \frac{\in r_p^2}{8\mu}\frac{\Delta P}{\tau\Delta x} \tag{25}$$

where ∈ represents void fraction (fractional open area), *u* the local center of mass velocity of pore fluid, r_p the pore radius, and, finally, μ solution viscosity. Whereas, total solute flux is demonstrated by the following two terms: contribution due to central mass fluid motion and solute diffusion distribution:

$$N_s = c_s u + J_s \tag{26}$$

where J_s represents solute flux. Based on Eq. (26), the solute diffusion term is derived from the concentration diffusion term, as to Fick's law, coupled with the pressure diffusion term, usually negligible. Since membrane pore dimension is affected by salt permeability; the previous equation is applicable when small pore dimension is less than 10 A^0. However, if pore dimension is equal or less

than 50 A^0, the diffusion process is disturbed by solute and membrane wall friction. For this reason, the total solute flux diffusion term was modified by adding solute and membrane friction force. The modified diffusion term is expressed accordingly:

$$J_s = m_{sw} c_s \left[-\left(\frac{\partial \mu_s}{\partial c_s} \right)_{T,p} \frac{dc_s}{dx} + F_{sm} \right] \tag{27}$$

where

$$m_{sw} = \frac{1}{f_{sw}} \tag{28}$$

$$F_{sm} = -f_{sm} \left(u_s - u_m^0 \right) = -f_{sm} u_s = -f_{sm} \frac{N_s}{c_s} \tag{29}$$

where F_{sm} represents friction force between solute and membrane pores, f_{sm} the frictional coefficient between solute and membrane pores, and u_s being defined as solute flux in membrane pores divided by membrane pore concentration, and u_m^0 the chemical reference pressure potential. According to the frictional model for dilute solution transport, $(\partial \mu_s / \partial c_s)_{T,P}$ is possibly substituted with RT/c_s, also F_{sm}, as represented in the equation shown in Eq. (29), thus the modified diffusion term becoming:

$$J_s = \frac{RT}{f_{sw} c_s} \frac{dc_s}{dx} - f_{sm} \frac{N_s}{c_s} \tag{30}$$

Therefore, total solute flux [Eq. (26)] replaced by the modified diffusion term is expressed as:

$$N_s = -D_e \frac{dc_s}{dx} + \frac{c_s}{b} u \tag{31}$$

where

$$D_e = \frac{RT}{f_{sw} b} \tag{32}$$

$$b = 1 + \frac{f_{sm}}{f_{sw}} \tag{33}$$

where D_e represents the effective diffusion coefficient of micropore solutes, b the frictional force ratio acting on the mobile solute — from membrane pores to friction force — and finally, f_{sw} the frictional coefficient between solute and water. Moreover, the concentration membrane profile during applied boundary conditions, as shown in Eqs. (34) and (35), is estimated in Eq. (30), N_s, u, b, and f_{sw} assumed to be constant.

$$\text{at} \quad x = 0, \qquad C_s = k_s' C_R \tag{34}$$

$$\text{at} \quad x = \tau\delta, \qquad C_s = k_s'' C_P \tag{35}$$

Thus, the membrane concentration profile is obtained:

$$c_s = \frac{N_s b}{u} + \frac{\left(k_s' C_R - k_s'' C_p \right) \exp\left(ux / bD_e \right)}{1 - \exp\left(u\tau\delta / bD_e \right)} \tag{36}$$

where k_s' and k_s'' represents the partition coefficient on high and low pressure sides of membranes, respectively, and $\tau\delta$ membrane pore length. When $N_s = (\in u)\, C_p$, Eq. (36) is thus expressed as:

$$c_s = \in C_p b + \frac{\left(k_s' C_R - k_s'' C_p \right) \exp\left(ux / bD_e \right)}{1 - \exp\left(u\tau\delta / bD_e \right)}, \quad 0 < x < \tau\delta \tag{37}$$

Finally, the salt rejection term is derived from Eq. (33) accordingly:

$$1 - R = \frac{C_p}{C_R} = \frac{k_s' C \exp\left(u\tau\delta / bD_e \right)}{k_s'' - b \in \exp\left(u\tau\delta / bD_e \right)} \tag{38}$$

Based on the classical finery-porous model, which takes total membrane concentration into consideration, Josson and Boesen (1975) were able to advance a new model, relying on only a fraction of water within membrane layer and pores, as well as taking tortuosity pores into account [64]. Subsequently, the modified rejection term was concluded accordingly:

$$1 - R = \frac{C_p}{C_R} = \frac{\exp\left(\in u \frac{\tau\delta}{\in} / bD_e \right)}{\frac{k_{sp}''}{k_{sp}'} - \frac{b}{k_{sp}'} \left[\exp\left(\in u \frac{\tau\delta}{\in} / bD_e \right) + 1 \right]} \tag{39}$$

Both Eqs. (38) and (39) are derived according to flat sheet membrane assumption, however, such terms are applicable to hollow fibers, as well. Hollow fiber walls are much thinner than flat sheet skin; therefore, such curvature is neglected, being considered identical to flat sheet membranes. In addition, Jonsson and colleagues note that such an equation supports transport mechanisms during membrane filtration, including solute membrane friction, pore dimension and distribution, and solute distribution [7,64]. In model utilization of dilute organic systems, results demonstrate that such an equation fails to address water flux decline description, compared to pure water flux. In order to correct and apply such an equation, pore dimension measurement is necessary [29].

4.2.3. Surface force pore flow model

The model was augmented to include a two-dimensional extension of the finery-porous model [65]. Moreover, such a model accounts for solute concentration both in axial position and radius, in contrast to the finery-porous model which considers only axial solute concentration gradients. The model provides excellent solute separation prediction for a wide range of inorganics and organics operating under various conditions [66]. However, the model fails to adequately predict the water flux ratio for particular dilute organics, causing substantial water flux decreases. With respect to systematic accord, the pore radius is necessarily reduced to predict force and measured water flux ratio. Basic model

assumptions include water transport via membrane pores by means of viscous flow, moreover, solute transport occurring by means of diffusion and convection within membrane pores. Both solute and solvent transport is investigated by means of interaction and friction forces, as well as chemical potential barrier layer gradients [32,62]. Thus, the ratio of water flux to pure water and rejection are represented by:

$$\frac{J_w}{J_{W0}} = \frac{2\int_0^{r_p} u r_p \, dr_p}{r_p{}^4 \Delta P} \tag{40}$$

$$R = \frac{1 - \int_0^{r_p} \left(\frac{\exp\left(u(r_p)\delta \frac{X_{sw}}{R_g T} \right) u(r_p) r_p}{1 + \frac{b(r_p)}{\exp\left(\frac{-\phi(r_p)}{R_g T} \right)} \left[\exp\left(u(r_p)\delta \frac{X_{sw}}{R_g T} \right) - 1 \right]} \right) dr_p}{\int_0^{r_p} u(r_p) r_p \, dr} \tag{41}$$

where X_{sw} is defined as $R_g T/D_{sm}$ and J_{W0} pure water flux.

4.3. Irreversible thermodynamics model

In order to understand transport mechanisms within membranes, discerning membrane structures is especailly vital, transport mechnisms being mainly dependent upon such structures. However, membrane structural features are not always available so irreversible thermodynamic models have been developed to overcome such problems [27,67,68]. The models are employed on the basis of irreversibility, dividing systems into smaller entities which replicate states at equilibrium [7]. A particular strength of such an approach is multicomponent system inclusion, used to predict membrane behavior. However, such models fail to elucidate actual transfer membrane mechanisms [29]. Moreover, the models, based on inherent membrane structures and properties, are not very consequential when optimizing separation. Currently, the models likewise fall short at effective water organic flux description for various dilutes [61].

4.3.1. Kedem–Katchalsky model

Kedem and Katchalsky (1958) developed a model for isothermal non-electrolyte systems in the absence of chemical reactions based on irreversible thermodynamic theories. The merits of such a model include minimal data requirement in addressing problems, as well as application ease, since parameters represent experimentally measurable quantities [68]. Furthermore, model coefficients (i.e., L_p, σ, and ω) rely less on degress of concentration [69]. Conversely, the model contains one limitation — the system being exclusively closed to equilibrium states [7]. Volume (J_v) and solute flux (J_s) are obtained by means of linear laws and onsager reciprocal relations (ORR) as expressed below:

$$J_w = L_P(\Delta p - \sigma \Delta \pi) \tag{42}$$

$$J_s = (c_s)_{ln}(1-\sigma)J_w + \omega \Delta \pi \tag{43}$$

where L_P represents the Staverman reflection coefficient and ω the solute permeability coefficient. An additional parameter important for transport models is the reflection coefficient. In such a case, the coupling of solute and solvent flux via membranes, usually employed to calculate solute rejection, is represented [50]. Specifically, solute rejection is expressed as following:

$$\frac{1}{R} = \frac{1}{\sigma} + \left(\frac{L_\pi}{L_p} - \sigma^2 \right) \left(\frac{L_p}{\sigma} \right) \pi_F \frac{1}{J_w} \tag{44}$$

where L_π is determined as $\bar{V}_m$, π_F representing feed side osmotic pressure.

4.3.2. Spiegler–Kedem model

Since various limitations in the Kedem–Katchalsky model exist, Spiegler and Kedem developed a model to overcome such inadequacy [7]. Included was the mention of three Kedem and Katchalsky model coefficients being less concentration-sensitive as to small volume flux and concentration gradient, conversely losing efficacy. Hence, to avoid concentration transport parameter dependence, local water (P_w) and solute (P_s) permeability, as well as reflection coefficients, were further defined [70]. The local phenomenological equations of solvent and solute flux, as well as the solute rejection coefficient, are represented accordingly:

$$J_w = -L_{ww}\bar{V}_w \left[\frac{dp}{dx} - \left(1 - \frac{L_{ws}}{L_{ww}} \frac{c_w}{c_s} \right) \frac{d\pi}{dx} \right] \tag{45}$$

$$J_s = \left(\frac{L_{ws}^2}{c_s L_{ww}} - \frac{L_{ss}}{c_s} \right) \frac{d\pi}{dx} + \frac{L_{sw}}{L_{ww}\bar{V}_w} J_w \bar{V}_w \tag{46}$$

$$R = \frac{\sigma \left[1 - e^{-J_v(1-\sigma)\Delta x / p_s} \right]}{1 - \sigma e^{-J_v(1-\sigma)\Delta x / p_s}} \tag{47}$$

where L_{ik} represents phenomenological coefficients as to linear laws of irreversible thermodynamics, $\bar{V}_w$ partial molar water volume, σ the reflection coefficient, and e electric ion charge. Such a model possesses meaningful RO membrane separation description and analysis due to concentration function independence. However, the model was simulated according to the "black box" model, limiting transport identification during filtration. In addition, the existence of ORR represents a further

constraint. In particular, ORR is beneficial in coefficient reduction; however, such a process is applicable only during appropriate conjugate flux and force identification, the existence of a wide linear range, and correlation with the equilibrium state [7].

4.3.3. Other models based on irreversible thermodynamics

An additional RO transport model, developed on irreversible thermodynamics though reducing ORR, is acknowledged [7]. Previous studies have revealed varying degrees of success in the use of dimensional analysis to correlate experimental RO membrane data. Mason and Lonsdale (1990) presented the statistical-mechanical membrane transport theory, pointing out that most RO membrane transport models are possibly derived from statistical-mechanical theories [71]. Furthermore, extended Stefan-Maxwell equations were revealed to illustrate total aqueous-organic solution flux (solute plus solvent) via membranes; the model indicating water flux reduction was partly due to frictional organic effects [61]. The model includes the form:

$$N_T = \frac{A\left\{\Delta P - \left[\pi(X_F) - \pi(X_P)\right]\right\}}{1 + W_S X_P} \tag{48}$$

where N_T represent total flux, X_F the solute mole fraction in feed water, X_p the solute mole fraction in permeate, and finally $W_s X_p$ the solute membrane friction term. Subsequently, an additional development is exposed by using the adsorption resistance term (R_{Ads}) to illuminate water flux decline in aqueous-organic systems. The model is rooted in the assumption that organics adsorbed on membranes influence high resistance of water flow through membranes. Moreover, such an equation has also been applied extensively in illuminating ultrafiltration membranes [72–74]. Water flux is represented as:

$$J_w = \frac{\Delta P - \Delta\pi}{R_m + R_{Ads}} \tag{49}$$

An alternative model is the frictional model, the equations within the model possessing notably uncomplicated physical interpretation. Components are assumed to move in a quasi-steady state in which driving force is balanced by frictional force gradient [7]. Frictional forces are assumed to be proportional to velocity differences between components and frictional drag origins [8,75–81]. The total force acting on water and salt are expressed accordingly:

$$F_w = (c_s / c_w) f_{sw}(u_w - u_s) + f_{wm}(u_w - u_m) \tag{50}$$

$$F_s = f_{sw}(u_s - u_w) + f_{sm}(u_s - u_m) \tag{51}$$

where F_s represents total force acting on salt and F_w total force acting on water. Thus, solvent and solute flux are expressed according to Eqs. (52) and (53), respectively.

$$J_w = \frac{\left(f_{sm} + f_{sw}\right)c_w^2}{d} F_w + \frac{f_{sw} c_w c_s}{d} F_s \tag{52}$$

$$J_s = \frac{f_{sw} c_w c_s}{d} F_w + \frac{\left(f_{wm} c_w + f_{sw} c_s\right)c_s}{d} F_s \tag{53}$$

Recently, modified concentration polarization model is developed since concentration polarization in the cross-flow RO process plays an important role inducing fouling. The development of this model starts from the principle of irreversible thermodynamics including theory of concentration polarization. As well as, the additional osmotic pressure arising from concentration polarization layer has been considered [82]. Thus, permeate flux in cross-flow RO process can be written as:

$$\Delta P = R_m v(x) + \frac{n\phi R_{gas} T R c_0}{D^2 \gamma} v(x)^2 \int_0^x v(x')\, dx' \tag{54}$$

where the additional osmotic pressure due to concentration polarization is determined as:

$$\Delta\pi_a = \frac{n\phi R_{gas} T R c_0}{D^2 \gamma} v(x)^2 \int_0^x v(x')\, dx' \tag{55}$$

where $v(x)$ represents permeate flux at x, n the number of ions in electrolyte, c_0 feed solute concentration, D the solute diffusion coefficient, γ the shear rate, x' the dummy integration variable, and $\Delta\pi_a$ the additional osmotic pressure.

5. Conclusions

To date, RO transport models and fouling mechanisms have been deliberated by numerous researchers over many decades. Nevertheless, fouling mechanisms, especially relating to NOM, have not been adequately elucidated. In particular, NOM fouling mechanisms, e.g., complex interactions between foulant-foulant and foulant-membrane surfaces due to various influential factors, simultaneously governing processes such as solution chemistry (e.g., pH, ionic strength and water hardness) [46,47,49–53]; membrane characteristics (e.g., hydrophobicity; surface/pore charge; (MWCO and morphology) [18,38,45–47,49,50]; operational conditions; inorganic presence and NOM characteristics (e.g., concentration, humic and non-humic fractions, charge, MW distribution) assist in explaining such lack of clarification [35]; physical condition such as pressure [49]. Additionally, the contribution of NOM fouling greatly depends on feed water properties, NOM characteristics, as well as manners of pretreatment. Thus, RO transport modeling during seawater desalination, especially NOM fouling development, has become a major challenge towards more effective fouling control and widespread RO application. Currently, RO transport models are categorized as to membrane surface structure composition according

to the following 3 types: diffusion-based, pore, and irreversible thermodynamic models [7]. In order to develop NOM fouling models for SWRO application, a number of studies have revealed challenges in solute system application, especially involving dilute organics. In particular, such models fail to adequately illuminate water flux decline [7,62]. Consequently, simplification is possibly accomplished by particular term introduction, impacting NOM fouling as to aforementioned models. However, several researchers have observed that such methods fail to adequately predict NOM fouling. Major difficulties with NOM fouling models are symbolized by lack of exact characterization (e.g., functional NOM group) and reliable linkage among feed water compositions, fouling rates, foulant transport and NOM characteristics. In addition, fouling model development depends on experimental verification methods and fouling potential, as well as existing operating conditions. Accordingly, specific NOM fouling models for SWRO application have not been fully developed to date. Therefore, to achieve high NOM fouling prediction accuracy as to SWRO application a holistic understanding of NOM fouling mechanisms, coupled with integrated experimentation, is required for NOM fouling model set-up.

6. Future direction of NOM fouling model

Predictive NOM fouling models, modified according to existing models, specifically require coefficient and modulating factor determination. In order to understand NOM fouling mechanisms, experimental data, i.e., intermolecular adhesion and hydrodynamic shear force, permeation drag, as well as membrane autopsy coupled with image analysis, is required. Correlation among factors effecting NOM fouling requires increased consideration due to the simultaneous and factor-varying nature of the process. Moreover, cross flow membrane filtration coupled with image analysis (i.e. AFM, TEM, CLSM and SEM), aiding in enhanced understanding of NOM fouling mechanisms and mass transport phenomena, is ideally applied to obtain essential model set-up information. Finally, NOM fouling models utilized for SWRO application are ideally modified by adding specific coefficients obtained from existing classic RO transport models. An additional aspect necessary in such deliberation is seawater NOM extraction. To date, all experiments designed for better understanding of fouling seawater mechanisms have been conducted by using extracted freshwater or synthetic NOM. Hence, high precision and accuracy is likely achieved via seawater NOM experimentation. Precisely, NOM characteristics and composition emanating from a variety of unique sources help to explain such likely results.

In brief, a clear understanding of NOM fouling mechanisms, as well as solutions preventing fouling problems during SWRO, are necessary for long-term fouling prevention. Moreover, in order to better understand NOM fouling mechanisms as a result of increasing concerns over the role and importance of humic substances as to various aspects of water chemistry, the need for a more concerted effort and approach has transpired. In the case in question, RO transport modeling, likely explaining transport particle phenomena including NOM, is essential in overcoming such problems.

Acknowledgements

This research was supported by a grant (07seaheroB02-01) from the Plant Technology Advancement Program funded by the Ministry of Land, Transport and Maritime Affairs of the Korean government.

Symbols

A — Solvent permeability coefficient in solution-diffusion model
A^* — A new permeability constant
A_m — Membrane surface area
a_i — Chemical activity of component i
B — Solute permeability coefficient
b — Ratio of the frictional force acting on the solute moving in a membrane pore to the friction force
C — Concentration from the bulk to the membrane interfacial
C_b — Bulk concentration
C_c — Concentrate solute concentration
C_F — Feed concentration
C_g — Gel layer concentration
C_i — Concentration of component i
C_m — Concentration at membrane surface
$(C_m)_{avg}$ — Logarithmic mean solute concentration in membrane
C_{ms} — Membrane solute concentration
C_p — Permeate concentration
C_R — Rejection concentration
C_{smf} — Solute membrane concentration which related to feed concentration
C_{smp} — Solute membrane concentration which related to permeate concentration
c_w — Solvent concentration
c_s — Local solute concentration per unit membrane volume
c_0 — Feed solute concentration
D — Solute diffusion coefficint
D_e — The effective diffusion coefficient of the solute in a micropore
D_s — Diffusion coefficient of the solute in the membrane
D_{sm} — Solute diffusion coefficient in the membrane
D_{sp} — Diffusivity of the solute of the solute in the membrane pore

D_w — Diffusion coefficient of the solvent in the membrane
D_{wn} — Water diffusivity in membrane
d — $d = f_{sm} + f_{wm}c_w + f_{sm}f_{sw}c_s + f_{sw}f_{wm}c_w$
e — Electric charge of the ion
F_s — Total force acting on salt
F_w — Total force acting on water
F_{sm} — Friction force between solute and membrane pore
f_{ik} — Frictional coefficient
f_{im} — Frictional coefficient
f_{sm} — Frictional coefficient between solute and membrane pore
f_{sw} — Frictional coefficient between solute and water
J_i — Fluxes
J_s — Solute flux
J_v — Volume flux; the sum of the diffusive solute and solvent fluxes (due to the Jw water flux gradient of chemical potential)
J_w — Flux of solvent due to the gradient of chemical potential with respect to membrane
J_{W0} — Pure water flux
K_1 — Water permeability coefficient
K_2 — Coupling coefficient describing pore flow
K_3 — Solute permeability coefficient
K_D — Distribution coefficient of the solute from the feed into the pore of membrane
K_{sm} — Partition coefficient defined as $K_{sm} = C_{smf}/C_F = C_{smp}/C_P$
k — Boltzman constant
k_s — Partition coefficient of the solute in the membrane with respect to the total membrane volume
k_s', k_s'' — Partition coefficient in the high and low pressure sides of membrane, respectively
k_{sp}', k_{sp}'' — Partition coefficient with respect to the pore volume in the high and low pressure sides of the membrane, respectively
L_{ik} — Phenomenological coefficients in the linear laws of irreversible thermodynamics
L_p — Staverman reflection coefficient
L_π — Determined from $\omega = (L_\pi/L_p - \sigma^2)$
m_{sw} — Mobility of solute in membrane
N_i — Flux (diffusion and convection) of component i with respect to the fixed coordinate (membrane)
N_s — Total solute flux
N_T — Total flux (solvent and solute) with respect to the fixed coordinate (membrane)
N_w — Water flux according to preferential sorption-capillary flow model
n — Number of ions in electrolyte
P — Transmembrane pressure
P_s — Solute permeability
P^0 — Reference pressure
Q_{tm} — Total solute adsorption in membrane
R — Rejection
R_{Ads} — Solute adsorption resistance
R_{cp} — Concentration polarization resistance
R_g — Gel layer resistance
R_{gas} — Gas constant
R_{in} — Internal pore fouling resistance
R_m — Membrane resistance
T — Temperature
r — Permeate water recovery
r_p — Pore radius
u — Local center-of-mass velocity of pore fluid
u_s — Defined as solute flux in membrane pore divided by concentration in membrane pore
u_m^0 — Chemical potential at the reference pressure
$\overline{V}_i$ — Partial molar volume of component i
$\overline{V}_w$ — Partial molar volume of water
V_F — Feed volume
V_w — Local water permeation velocity through the membrane
$v(x)$ — Permeate flux at point x
v_i — Average velocity
W_sX_p — Solute membrane friction term
X_F — Solute mole fraction in feed water
X_i — Forces
X_P — Solute mole fraction in permeate
X_{s2} — Mole fraction of the solute in the high pressure sides of the membrane
X_{s3} — Mole fraction of the solute in the low pressure sides of the membrane
X_{sw} — Defined as R_gT/D_{sm}

Greek

δ — Fouling layer thickness
ϕ — Local dissipation function
μ — Viscosity of solution
μ_w — Chemical potential of water
μ_i — Chemical potential component i
μ_i^0 — Chemical potential at reference pressure
μ_s — Chemical potential of solute
π — Osmotic pressure
π_a — Additional osmotic pressure
π_0 — Feed osmotic pressure
π_F — Osmotic pressure on the feed side
π_R — Osmotic pressure on the reject side
σ — Reflection coefficient
τ — Tortuosity of the membrane
$\tau\delta$ — Length of membrane pore
ω — Coefficient of solute permeability in Kedem-Katchalsky model
$\in$ — Void fraction (fractional open area) of the membrane

Subscripts

b — Bulk solution
m — Membrane

p — Pore
s — Solute (salt)
w — Solvent (water)

References

[1] Y.M. Kim, S.J. Kim, Y.S. Kim, S. Lee, I.S. Kim and J.H. Kim, Overview of systems engineering approaches for large scale seawater desalination plant with reverse osmosis networks. Desalination, 238 (2009) 312–332.

[2] Y.G. Lee, Y.S. Lee, J.J. Jeon, S. Lee, D.R. Yang, I.S. Kim and J.H. Kim, Artificial neural network model for optimizing operation of a seawater reverse osmosis desalination plant. Desalination, 247 (2009) 180–189.

[3] A.M. Hassan, S. Al-Jarrah, T.t Al-Lohibi, A. Al-Hamdan, L.M. Bakheet and M.M.I. Al-Amri, Performance evaluation of SWCC SWRO plants. Desalination, 74 (1989) 37–50.

[4] C. Fritzmann, J. Löwenberg, T. Wintgens and T. Melin, State-of-the-art of reverse osmosis, Desalination, 216 (2007) 1–76.

[5] A.W. Zularisam, A.F. Ismail and R. Salim, Behaviours of natural organic matter in membrane filtration for surface water — a review. Desalination, 194 (2006) 211–231.

[6] K.J. Howe, K.P. Ishida and M.M. Clark, Use of ATR/FTIR spectrometry to study fouling of microfiltration membranes by natural waters. Desalination, 147 (2002) 251–255.

[7] M. Soltanieh and W.N. Gill, Review of reverse osmosis membranes and transport models. Chem. Eng. Commun., 12 (1981) 279–363.

[8] C. Bhattacharjee and P. Bhattacharya, Flux decline behavior with low molecular weight solutes during ultrafiltration in an unstirred batch cell. J. Membr. Sci., 72 (1992) 149.

[9] G. Jonsson, Overview of theories for water and solute transport in UF/RO membranes. Desalination, 35 (1980) 21.

[10] A. Ghani, R. Al-Rasheed and M.A. Javeed, Studies on organic foulants in the seawater feed of reverse osmosis plants of SWCC. Desalination, 132 (2000) 217–232.

[11] M.A.K. Al-Sofi, Seawater desalination—SWCC experience and vision. Desalination, 135 (2001) 121–139.

[12] A. Butterworth-Heinemann, Seawater: Its Composition, Properties and Behaviour. Linacre House, Jordan Hill, Oxford, 2nd ed., 1995.

[13] The Oxford Companion to Ships and the Sea. Oxford University. P. Kemp, ed., Retrieved Oxford University Press, 1988.

[14] R.J. Petersen, Composite reverse osmosis and nanofiltration membranes. J. Membr. Sci., 83 (1993) 81–150.

[15] D.E. Potts, R.C. Ahlert and S.S. Wang, A critical review of fouling of reverse osmosis membranes. Desalination, 36 (1981) 235–264.

[16] L. Norman N., F. Anthony G., H.W.S. Winston and M. Takeshi, Advance Membrane Technology and Applications. John Wiley & Sons, New Jersey, 2008.

[17] Desalination by reverse osmosis. http://www.oas.org/usede/publications/unit/oea59e/ch20.htm, accessed on November 10, 2009.

[18] H.Y. Ju, Role of foulant-membrane interactions in organic fouling of RO membranes, MSc thesis, 2009.

[19] C.E. Reid and E.J. Breton, Water and ion flow across cellulosic membranes. J. Appl. Polym. Sci., 1 (1959) 133.

[20] S.J. Kim, Y.G. Lee, K.H. Cho, Y.M. Kim, S. Choi, I.S. Kim, D.R. Yang and J.H. Kim, Site-specific raw seawater quality impact study on SWRO process for optimizing operation of the pressurized step. Desalination, 238 (2009) 140–157.

[21] J.M. Veza, Desalination in the Canary Islands: an update. Desalination, 133 (2001) 259–270.

[22] S.J. Kim, S. Oh, Y.G. Lee, M.G. Jeon, I.S. Kim and J.H. Kim, A control methodology for the feed water temperature to optimize SWRO desalination process using genetic programming. Desalination, 247 (2009) 190–199.

[23] R. Petersen and J. Cadote, Thin film composite reverse osmosis membranes. Handbook of Industrial Membrane Technology, M. Porter, ed., Noyes Publications, Park Ridge, NJ, 1990, pp. 307–348.

[24] W. Pusch, Measurement techniques of transport through membranes. Desalination, 59 (1986) 105.

[25] G.P. Simon and C. Calmon, Experimental methods for the determination of non-transport properties of membranes. Desalination, 59 (1986) 61.

[26] G. Mierle and R. Ingram, The role of humic substances in the mobilization of mercury from watersheds. Water Air Soil Pollut., 56 (1991) 349.

[27] S.K. Edward, J. Chian, P. Chen, P.X. Sheng, Y.P. Ting and L.K. Wang, Reverse Osmosis Technology for Desalination Handbook of Environmental Engineering. Vol. 5: Advanced Physicochemical Treatment Technologies. The Humana Press Inc., Totowa, NJ, 2007.

[28] S. Lee, W.S. Ang and M. Elimelech, Fouling of reverse osmosis membranes by hydrophilic organic matter: implications for water reuse. Desalination, 187 (2006) 313–321.

[29] S. Lee and M. Elimelech, Salt cleaning of organic-fouled reverse osmosis membranes. Wat. Res., 41 (2007) 1134–1142.

[30] W. Luck, Contributions to the desalination membrane mechanism by studies of interactions in aqueous solutions and in polymer hydration. Desalination, 62 (1987) 19.

[31] R. Cheng, J. Glater, J.B. Neethling and M.K. Stenstrom, The effects of small halocarbons on RO membrane performance. Desalination, 85 (1991) 33.

[32] D. Bhattacharyya and A. Kothari, Separation of Hazardous Organics by Low Pressure Membranes: Treatment of Soil-Wash Rinse-Water Leachates. EPA Report, Cooperative Agreement No. CR814491, Submitted 1991.

[33] D. Bhattacharyya and M. Williams, Separation of Hazardous Organics by Low Pressure Reverse Osmosis Membranes – Phase II, Final Report. EPA Report, EPA/600/2-91/045, 1992.

[34] J. McN. Sieburth and A. Jensen, Studies on algal substances in the sea I. Gelbstoff (humie material) in terrestrial and marine waters. J. Exp. Mar. Biol. Ecol., 2 (1968) 174–189.

[35] S.K. Hong and M. Elimelech, Chemical and physical aspects of natural organic matter (nom) fouling of nanofiltration membranes. J. Membr. Sci., 132 (1997) 159.

[36] C. Jucker and M.M. Clark, Adsorption of aquatic humic substances on hydrophobic ultrafiltration membranes. J. Membr. Sci., 97 (1994) 37–52.

[37] L. Braeken, R. Ramaekers, Y. Zhang, G. Maes, B. Van Der Bruggen and C. Vandecasteele, Influence of hydrophobicity on retention in nanofiltration of aqueous solutions containing organic compounds. J. Membr. Sci., 252 (2005) 195–203.

[38] R. Cheng, J. Glater, J.B. Neethling and M.K. Stenstrom, The effects of small halocarbons on RO membrane performance. Desalination, 85 (1991) 33.

[39] M. Elimelech, X. Zhu, A.E. Childress and S. Hong, Role of membrane surface morphology in colloidal fouling of cellulose acetate and composite aromatic polyamide reverse osmosis membranes, J. Membr. Sci., 127 (1997) 101–109.

[40] E.M. Vrijenhoek, S. Hong and M. Elimelech, Influence of membrane surface properties on initial rate of colloidal fouling of reverse osmosis and nanofiltration membranes. J. Membr. Sci., 188 (2001) 115–128.

[41] W.R. Bowen, N. Hilal, R.W. Lovitt and C.J. Wright, A new technique for membrane characterisation: Direct measurement of the force of adhesion of a single particle using an atomic force microscope. J. Membr. Sci., 139 (1998) 269–274.

[42] A.E. Childress and S.S. Deshmukh, Effect of humic substances and anionic surfactants on the surface charge and performance of reverse osmosis membranes. Desalination, 118 (1998) 167–174.

[43] Y. Shim, H.J. Lee, S. Lee, S.H. Moon and J. Cho, Effects of natural organic matter and ionic species on membrane surface charge, Environ. Sci. Technol., 36 (2002) 3864–3871.

[44] J.A. Brant, K.M. Johnson and A.E. Childress, Examining the

electrochemical properties of a nanofiltration membrane with atomic force microscopy. J. Membr. Sci., 276 (2006) 286–294.
[45] B. Van der Bruggen, J. Schaep, D. Wilms and C. Vandecasteele, Influence of molecular dimension, polarity and charge on the retention of organic molecules by nanofiltration. J. Membr. Sci., 156 (1999) 29–41.
[46] A. Al-Amoudi and R. W. Lovitt, Fouling strategies and the cleaning system of NF membranes and factors affecting cleaning efficiency. J. Membr. Sci., 303 (2007) 4–28.
[47] B. Van der Bruggen, L. Braeken and C. Vandecasteele, Flux decline in nanofiltration due to adsorption of organic compounds. Sep. Purif. Technol., 29 (2002) 23–31.
[48] L.F. Song and M. Elimelech, Particle deposition onto a permeable surface in laminar-flow. J. Colloid Interface Sci., 173 (1995) 165–180.
[49] I. le Rouxa, H.M. Kriegb, C.A. Yeatesa and J.C. Breytenbacha, Use of chitosan as an antifouling agent in a membrane bioreactor. J. Membr. Sci., 248 (2005) 127–136.
[50] A.I. Schaäfer, A. Pihlajamaki, A.G. Fane, T.D. Waite and M. Nyström, Natural organic matter removal by nanofiltration: effects of solution chemistry on retention of low molar mass acids versus bulk organic matter. J. Membr. Sci., 242 (2004) 73–85.
[51] A.E. Childress and M. Elimelech, Effect of solution chemistry on the surface charge of polymeric reverse osmosis and nanofiltration membranes. J. Membr. Sci., 119 (1996) 253–268.
[52] M. Elimelech, W.H. Chen and J.J. Waypa, Measuring the zeta (electrokinetic) potential of reverse osmosis membranes by a streaming potential analyzer. Desalination, 95 (1994) 269–286.
[53] W. Yuan and A.L. Zydney, Humic acid fouling during microfiltration. J. Membr. Sci., 157 (1999) 1–12.
[54] L.D. Nghiem and P.J. Coleman, NF/RO filtration of the hydrophobic ionogenic compound triclosan: transport mechanisms and the influence of membrane fouling, Sep. Purif. Technol., 62 (2008) 709–716.
[55] T.-U. Kim, J.E. Drewes, R.S. Summer and G. Amy, Solute transport model for trace organic neutral and charged compounds through nanofiltration and reverse osmosis membranes, Water Res., 41 (2007) 3977–3988.
[56] S. Lee and R.M. Lueptow, Reverse osmosis filtration for space mission wastewater: membrane properties and operating conditions. J. Membr. Sci., 182 (2001) 77–90.
[57] H. Lonsdale, U. Merten and R. Riley, Transport properties of cellulose acetate osmotic membranes. J. Appl. Polym. Sci., 9 (1965) 1341.
[58] R.L. Riley, H.K. Lonsdale, C.R. Lyons and U. Merten, The preparation of ultrathin reverse osmosis membranes and the attainment of 'theoretical' salt rejection. J. Appl. Polym. Sci., 11 (1967) 2143–2158.
[59] M.E. Williams, J.A. Hestekin, C.N. Smothers and D. Bhattacharyya, Separation of organic pollutants by reverse osmosis and nanofiltration membranes: mathematical models and experimental verification. Ind. Eng. Chem. Res., 38 (1999) 3683–3695.
[60] H. Burghoff, K. Lee and W. Pusch, Characterization of transport across cellulose acetate membranes in the presence of strong solute-membrane interactions. J. Appl. Polym. Sci., 25 (1980) 323.
[61] T. Sherwood, P. Brian and R. Fisher, Desalination by reverse osmosis. Indust. Eng. Chem. Fundam., 6 (1967) 2.
[62] M.E. Williams, A Brief Review of Reverse Osmosis Membrane Technology, EET Corporation and Williams Engineering Series Company, Inc., Albany, Kentucky, 2003.
[63] Y. Zhao, Modeling of membrane solute mass transfer in NF/RO membrane systems. Ph.D Thesis, Department of Civil and Environmental Engineering, College of Engineering and Computer Science, University of Central Florida, Orlando, Florida, 2004.
[64] G. Jonsson and C. Boesen, Water and solute transport through cellulose acetate reverse osmosis membranes. Desalination, 17 (1975) 145.
[65] T. Matsuura and S. Sourirajan, Reverse osmosis transport through capillary pores under the influence of surface forces. Indus. Eng. Chem. Process Design Dev., 20 (1981) 273–279.
[66] H. Mehdizadeh, J. Dickson and P. Eriksson, Temperature effects on the performance of thin-film composite, aromatic polyamide membranes. Indus. Eng. Chem. Res., 28 (1989) 814–819.
[67] J.W. Lorimer, Phenomenological coefficients and frames of reference for transport processes in liquids and membranes: Part 3, Theory of convective contributions to isothermal and nonisothermal transport in ionic membranes. J. Membr. Sci., 14 (1983) 275.
[68] L.F. de1 Castillo and E.A. Mason, Generalization of membrane reflection coefficients for nonideal, nonisothermal, multicomponent systems with external forces and viscous flow. J. Membr. Sci., 28 (1986) 229.
[69] O. Kedem and A. Katchalsky, Thermodynamic analysis of the permeability of biological membranes to non-electrolytes. Biochim. Biophys. Acta, 27 (1958) 229.
[70] J. Jagur-Grodzinski and O. Kedem, Transport coefficients and salt rejection in uncharged hyperfiltration membranes. Desalination, 1 (1966) 327–341.
[71] K. Spiegler and O. Kedem, Thermodynamics of hyperfiltration (reverse osmosis): criteria for efficient membranes. Desalination, 1 (1966) 311.
[72] E.A. Mason and H.K. Lonsdale, Statistical mechanical theory of membrane transport. J. Membr. Sci., 51 (1990) 1.
[73] S. Nakatsuka and A. Michaels, Transport and separation of proteins by ultrafiltraion through sorptive and non-sorptive membranes. J. Membr. Sci., 69 (1992) 189.
[74] C. Bhattacharjee and P. Bhattacharya, Prediction of limiting flux in ultrafiltration of Kraft black liquor. J. Membr. Sci., 72 (1992) 137.
[75] S. Sourirajan, The mechanism of demineralization of aqueous sodium chloride solutions by flow under pressure through porous membranes. Ind. Eng. Chem. Fundam., 2 (1963) 51.
[76] G.D. Mehta, T.F. Morse, E.A. Mason and M.H. Daneshpajooh, Generalized Nernst-Planck and Stefan-Maxwell equations for membrane transport. J. Chem. Phys., 64 (1976) 3917.
[77] E.A. Mason and L.A. Viehland, Statistical-mechanical theory of membrane transport for multicomponent systems: Passive transport through open membranes. J. Chem. Phys., 68 (1978) 3562.
[78] E.A. Mason and L.F. de1 Castillo, The role of viscous flow in theories of membrane transport. J. Membr. Sci., 23 (1985) 199.
[79] A. Katchalsky and O. Kedem, Thermodynamics of flow processes in biological systems. Biophys. J., Suppl. 2 (1962) 53.
[80] O. Kedem and A. Katchalsky, A physical interpretation of the phenomenological coefficients of membrane permeability. J. Gen. Physiol., 45 (1961) 143.
[81] M.H. Daneshpajooh, E.A. Mason, E.H. Bresler and R.P. Wendt, Equations for membrane transport. Experimental and theoretical tests of the frictional model. Biophys. J., 15 (1975) 591.
[82] L. Song and S. Yu, Concentration polarization in cross-flow reverse osmosis. AIChE J., 45(1999) 921–928.